4340–4353 *Nucleic Acids Research, 2016, Vol. 44, No. 9* *Published online 16 March 2016*
doi: 10.1093/nar/gkw167

Tat-dependent production of an HIV-1 TAR-encoded miRNA-like small RNA

Alex Harwig[1], Aldo Jongejan[2], Antoine H. C. van Kampen[2,3], Ben Berkhout[1] and Atze T. Das[1,*]

[1]Laboratory of Experimental Virology, Department of Medical Microbiology, Center for Infection and Immunity Amsterdam (CINIMA), Academic Medical Center, University of Amsterdam, Meibergdreef 15, 1105 AZ Amsterdam, The Netherlands, [2]Bioinformatics Laboratory, Department of Clinical Epidemiology, Biostatistics and Bioinformatics, Academic Medical Center, University of Amsterdam, Meibergdreef 15, 1105 AZ Amsterdam, The Netherlands and [3]Biosystems Data Analysis, Swammerdam Institute for Life Sciences, University of Amsterdam, Science Park 904, 1098 XH Amsterdam, The Netherlands

Received January 23, 2015; Revised March 02, 2016; Accepted March 03, 2016

ABSTRACT

Evidence is accumulating that retroviruses can produce microRNAs (miRNAs). To prevent cleavage of their RNA genome, retroviruses have to use an alternative RNA source as miRNA precursor. The trans-acting responsive (TAR) hairpin structure in HIV-1 RNA has been suggested as source for miRNAs, but how these small RNAs are produced without impeding virus replication remained unclear. We used deep sequencing analysis of AGO2-bound HIV-1 RNAs to demonstrate that the 3′ side of the TAR hairpin is processed into a miRNA-like small RNA. This ∼21 nt RNA product is able to repress the expression of mRNAs bearing a complementary target sequence. Analysis of the small RNAs produced by wild-type and mutant HIV-1 variants revealed that non-processive transcription from the HIV-1 LTR promoter results in the production of short TAR RNAs that serve as precursor. These TAR RNAs are cleaved by Dicer and processing is stimulated by the viral Tat protein. This biogenesis pathway differs from the canonical miRNA pathway and allows HIV-1 to produce the TAR-encoded miRNA-like molecule without cleavage of the RNA genome.

INTRODUCTION

MicroRNAs (miRNAs) are small RNAs (∼21 nt in size) that have important post-transcriptional regulatory roles by targeting messenger RNAs (mRNAs) for cleavage or translational repression (1). In the canonical pathway, miRNAs are derived from stem-loop RNA structures within long primary miRNA transcripts (pri-miRNAs). Recognition and cleavage of the pri-miRNA into a precursor miRNA (pre-miRNA) hairpin is mediated by the nuclear microprocessor complex that consists of at least two subunits: the ribonuclease (RNAse) III Drosha and the double-stranded RNA (dsRNA)-binding protein DGCR8 (DiGeorge syndrome critical region protein 8) (2,3). The stem-loop structure in the pri-miRNA is recognized by DGCR8 and Drosha cleaves both strands at ∼11 base pairs (bp) from the base of the stem (4). The pre-miRNA is exported to the cytoplasm and further processed by the RNase III Dicer (5,6). Dicer cleaves both strands of the pre-miRNA at ∼2 helical turns (∼21 nt) from the Drosha cleavage sites (1,7). The guide strand of the double-stranded miRNA is loaded into the Argonaute2 (AGO2) protein, which is part of the RNA-induced silencing complex (RISC) to target a complementary mRNA, while the passenger strand is degraded (8,9).

Several DNA viruses encode miRNAs, including viruses of the Herpesviridae, Polyomaviridae and Adenoviridae (10). For retroviruses like human immunodeficiency virus type-1 (HIV-1), it has remained controversial whether they encode miRNAs. Retroviruses are RNA viruses with a DNA replication intermediate that is transcribed by RNA polymerase II (RNAP II) in the nucleus. Microprocessor and subsequently Dicer will thus be able to access and process the viral RNAs. Canonical production of an avian leukosis virus subgroup J (ALV-J) encoded miRNA has indeed been suggested (11). However, such canonical miRNA processing is expected to lead to RNA genome cleavage and inhibition of retrovirus replication (12). Recent studies revealed that bovine leukemia virus (BLV) (13,14), bovine foamy virus (BFV) (15) and simian foamy virus (SFV) (16) use a non-canonical pathway to produce miRNAs. These retroviruses encode sub-genomic RNA polymerase III (RNAP III) transcripts that serve as pre-miRNAs, thus avoiding degradation of their RNA genome. Several studies described miRNAs derived from the HIV-1 transacting

*To whom correspondence should be addressed. Tel: +31 20 5663396; Email: a.t.das@amc.uva.nl

responsive (TAR) RNA domain (17–21). These TAR miRNAs may prevent apoptosis of the infected cell for the purpose of increased virus production (22,23) or induce chromatin remodelling to induce latency (18,21). The relevance of these findings was however disputed because it was not clear how these miRNAs could be produced without impeding virus production (24–26).

The 57-nt TAR element is present at the 5′ and 3′ end of all HIV-1 RNA transcripts and can fold a stable hairpin structure (Figure 1). The best-studied function of the 5′ TAR element is its essential role in the activation of transcription from the long terminal repeat (LTR) promoter in the proviral genome (27). In the absence of the viral Tat transactivator protein, RNAP II initiates transcription but the nascent TAR RNA structure causes pausing and premature termination of transcription (28). This non-processive transcription results in the synthesis of short TAR transcripts (29–31) (Figure 1A). Upon binding of Tat and the cellular positive transcription elongation factor b (P-TEFb) complex to TAR RNA, RNAP II is phosphorylated, which activates processive transcription and production of full-length viral RNAs (29).

MiRNAs are loaded in the AGO2/RISC complex to exert their regulatory function. We used this important characteristic to identify HIV-1 encoded miRNAs by deep sequencing of AGO2-bound viral RNAs. This analysis revealed that the TAR element encodes a miRNA-like small RNA that originates from the 3′ side of the hairpin. We used wild-type (wt) HIV-1 and TAR and Tat-mutated virus variants to investigate how this small RNA molecule is produced and the role of the Tat protein.

MATERIALS AND METHODS

Cell culture, transfection and infection

Human Embryonic Kidney 293T, HCT-116 and HCT-116-Ex5 cells (32) were cultured as monolayer in Dulbecco's modified Eagle's medium (Invitrogen) supplemented with 10% fetal bovine serum, penicillin (100 U/ml) and streptomycin (100 μg/ml) at 37°C and 5% CO_2. Cells (5×10^6 cells) were cultured in 25 cm^2 flasks and transfected with 5 μg HIV plasmid DNA using lipofectamin2000 (Life technologies). When indicated, cells were cultured with 1 μg/ml doxycycline (dox; Sigma D-9891). At 2 days after transfection, virus production in culture medium samples was measured using CA-p24 ELISA (33). CD4-enriched human peripheral blood mononuclear cells (PBMC) were isolated from four donors, pooled, cultured and activated with IL-2 and phytohemagglutinin for 3 days, as described previously (35). 10×10^6 cells in 5 ml culture medium were infected with 293T-produced wt HIV-1 virus (corresponding to 40 ng CA-p24). After culturing the cells for 48 h, small intracellular RNA was isolated and analysed by northern blotting.

Plasmid constructs

The HIV-1 molecular clone pLAI (34) and the dox-dependent derivatives HIV-rtTA-Tat^{wt} (35), HIV-rtTA-TAR^{mut}-Tat^{stop} (35) and HIV-rtTA-$\Delta TAR^{5'+3'}$ (ER2-Tat^{Y26A} variant in (36)) were previously described.

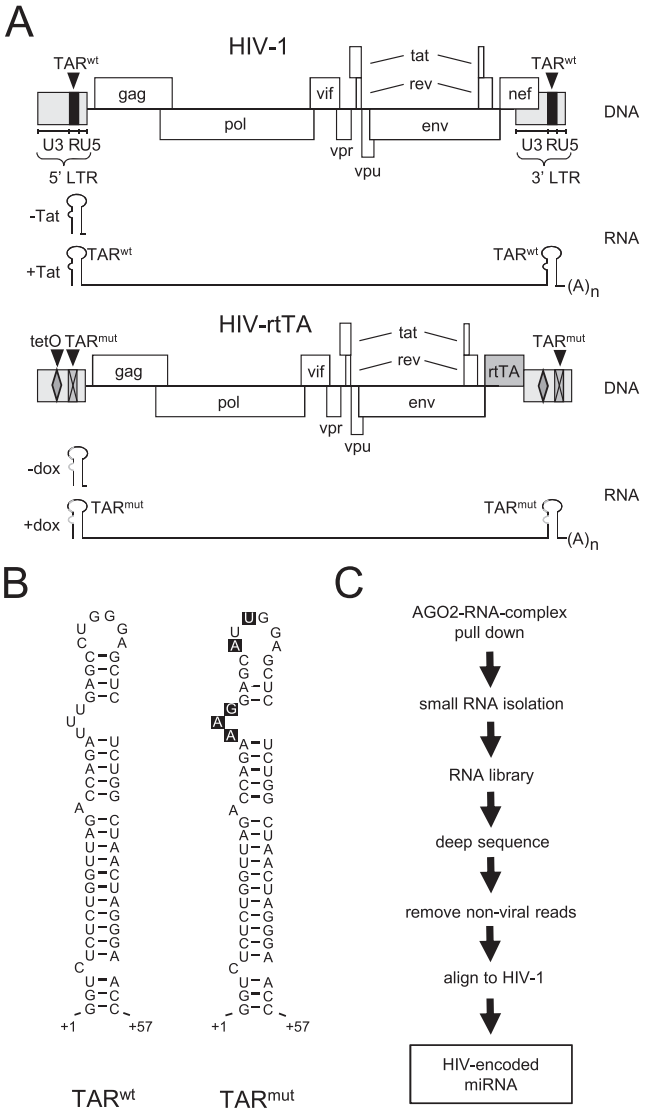

Figure 1. Experimental design. (**A**) A schematic of the HIV-1 and HIV-rtTA genome is shown, with the LTR subdivided in U3, R and U5 domains. In HIV-rtTA, the Tat-TAR axis of transcription regulation was inactivated by multiple nucleotide substitutions in the bulge and loop sequences of TAR (TAR^{mut}, crossed boxes). Transcription and replication of the virus were made dox dependent by the introduction of tetO elements in the U3 region of the LTR promoter and replacement of the nef gene by the rtTA gene. The short TAR-only and full-length RNA molecules produced by non-processive (in the absence of Tat [-Tat] or dox [-dox]) and processive transcription (in the presence of Tat [+Tat] or dox [+dox]), respectively, are shown. (**B**) Structure of the TAR hairpin of HIV-1 (TAR^{wt}) and HIV-rtTA (TAR^{mut}). The bulge and loop mutations present in TAR^{mut} are boxed in black. (**C**) Strategy used to identify AGO2-bound viral RNAs.

HIV-rtTA-$\Delta TAR^{5'}$ was constructed by replacing the 3′ BamHI – BglI fragment of HIV-rtTA-$\Delta TAR^{5'+3'}$ with the corresponding fragment of HIV-rtTA-Tat^{Y26A}. HIV-rtTA-$\Delta TAR^{3'}$ was constructed by replacing the 3′ BamHI – BglI fragment of HIV-rtTA-Tat^{Y26A} with the corresponding fragment of HIV-rtTA-$\Delta TAR^{5'+3'}$. For mutation of the Sp1 sites in the 3′ LTR, this region was PCR-amplified with primers mutSp1 (GAAA***GTCGAC***AGAATTCCG TGGCCTGTTCTCGAGGAATTCCTCGAGAGCCC

TCAGATGCTGCA; mutated nucleotides underlined; SalI site in italics and bold) and C(N1) (antisense primer annealing to the U5 region) (37), and with pBlue3′LTRext-ΔU3-rtTA$_{F86Y\ A209T}$-2ΔtetO, which includes Env, rtTA and 3′ LTR sequences of the HIV-rtTA genome (38), as template. The PCR product was digested with SalI and HindIII, and used to replace the corresponding 3′ LTR fragment in pBlue3′LTRext-ΔU3-rtTA$_{F86Y\ A209T}$-2ΔtetO. The BamHI-BglI fragment of the resulting shuttle plasmid pBlue3′LTRext-ΔU3-rtTA$_{F86Y\ A209T}$-2ΔtetO-mutSp1 was used to replace the corresponding Env-rtTA-3′LTR sequences in HIV-rtTA-ΔTAR$^{5'+3'}$, which resulted in plasmid HIV-rtTA-ΔTAR$^{5'}$-mutSp1$^{3'}$.

HIV-Tat^{stop} was constructed by replacing the NcoI-BamHI fragment of HIV-1 pLAI with the NcoI-BamHI fragment from HIV-rtTA-TAR^{mut}-Tat^{stop}. For the construction of HIV-rtTA-Tat^{stop}-TAR^{wt}, mutagenesis PCR was performed using primers tTA3 (35) and wt-TAR CAGA***GAGCTC***CCAGGCTCAAATCTGGT; mutated nucleotides underlined; SacI site in italics and bold and HIV-rtTA as template. The resulting fragment was digested with SacI and NdeI, and used to replace the corresponding fragment in pBlue3′LTRext-ΔU3-rtTA$_{F86Y\ A209T}$-2ΔtetO. The BamHI-BglI Env-rtTA-3′LTR fragment of the resulting plasmid pBlue3′LTRext-ΔU3-rtTA$_{F86Y\ A209T}$-2ΔtetO-TAR^{wt} was used to replace the corresponding sequences in HIV-rtTA-Tat^{stop}, which resulted in HIV-rtTA-Tat^{stop}-3′TAR^{wt}. Subsequently, the LTR region in pBlue3′LTRext-ΔU3-rtTA$_{F86Y\ A209T}$-2ΔtetO-TAR^{wt} was PCR amplified using the primers U3-Xba-Not and U5-Nar (36), and the produced fragment was used to replace the corresponding NotI-NarI fragment in HIV-rtTA-Tat^{stop}-3′TAR^{wt}, which resulted in HIV-rtTA-Tat^{stop}-TAR^{wt}.

A three-step mutagenesis PCR protocol (39) was used for the construction of HIV-Tat^{stop}-TAR$^{\Delta bulge}$. PCR 1 was performed using the primers tTA3 and TAR-noBulge-rev (GAGAGCTCCCAGGCTCTCTGGTCTAACCAGA), and pLAI as template. PCR 2 was performed using the primers TAR-noBulge-fw (CTCTCTGGTTAGACCAGAGAGCCTGGGAGCTC) and pLAI3′seq (36), and the pLAI template. The PCR 1 and PCR 2 products were purified and combined to function as template in PCR 3, using the outer primers tTA3 and pLAI3′seq. The resulting LTR-encoding fragment (with the TAR$^{\Delta bulge}$ sequence) was used to replace the XhoI-AatII 3′ LTR fragment in HIV-Tat^{stop}, resulting in HIV-Tat^{stop}-TAR$^{3'\Delta bulge}$. The PCR 3 fragment was also used as template in a PCR with primers U3-Xba-Not and U5-Nar. The product was used to replace the XbaI-NarI 5′ LTR fragment in HIV-TAR$^{3'\Delta bulge}$-Tat^{stop}, which resulted in the HIV-Tat^{stop}-TAR$^{\Delta bulge}$ mutant with the TAR$^{\Delta bulge}$ mutation in both the 5′ and 3′ LTR.

The plasmid pLTR-2ΔtetO-luc^{ff}, in which the LTR promoter region from HIV-rtTA is coupled to the firefly luciferase gene, was previously described (36). The plasmid pGL3-miR-TAR-3p^{target} was constructed by insertion of six copies of the 21-nt sequence complementary to miR-TAR-3p (TGGCTAACTAGGGAACCCACT) between the EcoRI and PstI sites in the 3′untranslated region downstream of the firefly luciferase gene in the pGL3 plasmid (Promega).

Small RNA library preparation and SOLiD deep sequencing

293T cells (5 × 10^6 cells per 25 cm^2 flask) were co-transfected with 5 μg AGO2-FLAG plasmid (40) and 20 μg HIV-1 (34), HIV-rtTA-Tat^{wt} (35) or pBluescript plasmid (Stratagene), and cultured for 48 h. HIV-rtTA transfected cells were cultured with 1 μg/ml dox (Sigma; D-9891). AGO2-bound small RNAs were isolated by immunoprecipitation using anti-FLAG M2 affinity gel (Sigma; A2220) as previously described (41). Five microgram RNA was loaded on a denaturing 15% PAGE gel for size fractionation and the 15–55 nt RNA fragments were isolated using a spin column (Ambion). The quality of the RNA was assayed on a Bioanalyzer 2100 (Agilent) using a small RNA chip. The SOLiD Small RNA Library Preparation protocol (Applied biosystems) was used to prepare an RNA library that was subsequently analysed using the SOLiD Wildfire system (Applied biosystems).

Bioinformatics

The SOLiD colorspace reads obtained for HIV-1 and HIV-rtTA samples were analysed with LifeScope Genomic Analysis Software version 2.5 (Applied biosystems) using the small RNA pipeline and the highest quality value, allowing no mismatches. First, the libraries were mapped against the human genome filter-sequences (supplied with LifeScope) and miRBase (version 21; http://www.mirbase.org) to identify reads generated from cellular or irrelevant sources. The remaining reads were mapped to the reference sequence of HIV-1 LAI or HIV-rtTA. Reads that were also observed with the pBluescript-transfected 293T cells were occluded.

Northern blot analysis

293T and HCT-116 (wt or Ex5) cells cultured in 25 cm^2 flasks were transfected with 5 μg HIV-1, HIV-rtTA or pLTR-2ΔtetO-luc^{ff} plasmid. When indicated, cells were co-transfected with 50 or 500 ng Tat expressing plasmid (pTAT; (35)) or 1 μg/ml dox was added to the culture medium. Cells were harvested after 48 h and small intracellular RNA was isolated with the mirVana miRNA isolation kit (Ambion). Isolated RNA (2 μg HIV-rtTA or 4 μg LAI RNA sample) was analysed by northern blotting as previously described (20). To check for equal sample loading, the 5S rRNA and tRNA bands were visualized by ethidium bromide staining. The LNA oligonucleotide 5′-AAGCAGTGGGTTCCCTAGTTAG-3′ (LNA-positions underlined) complementary to the 3′ end of the TAR hairpin was used as probe to detect miR-TAR-3p and TAR-containing RNAs.

Luciferase assay

293T cells were cultured in 0.5 ml medium in 1-cm^2 wells to 50% confluence and transfected with 50 ng pGL3-miR-TAR-3p^{target} or pGL3-shRT5^{target} (42), 0.5 ng pRL-CMV (Promega), 0–1250 ng HIV-1, HIV-Tat^{stop}, HIV-TAR$^{\Delta bulge}$-Tat^{stop} or shRNA-RT5 expression plasmid (42) and 0–1250 ng empty pcDNA3 vector (to complete the DNA to 1300 ng in total) using lipofectamin2000 (Life technologies). After culturing the cells for 48 h, the cells were lysed in 75 μl

Passive Lysis Buffer (Promega) and the firefly and renilla luciferase activities were measured with the Dual-Luciferase Reporter Assay System (Promega). The firefly luciferase activity was normalized to the renilla luciferase activity to correct for experimental variation.

Characterization of Dicer bound RNAs

293T cells (5×10^6 cells per 25 cm^2 flask) were transfected with 4 μg HIV-Tat^{stop} plasmid and 1 μg FLAG-tagged Dicer plasmid (Addgene plasmid 19881 (43)) or 1 μg FLAG-tagged hepatitis C virus (HCV) E2 plasmid (44). At 48 h post-transfection, Dicer and E2 bound small RNAs were isolated by immunoprecipitation using anti-FLAG M2 affinity gel (Sigma; A2220) and analysed in a similar way as previously described for AGO2-binding RNAs (45). Briefly, RNAs were polyadenylated using the Poly(A) Polymerase Tailing Kit (Epicentre Biotechnologies) and reverse transcribed into cDNA using an oligo-dT_{30}-adaptor primer. The cDNA products were PCR amplified with the forward primer (TGCGGATCCCCGGTCTCTCTGGTTAGACCAGA; TAR +1/+21 sequence underlined) or (TGGGATGAGGTAGTAGGTTGTATA; Let-7A-1 +1/+19 sequence underlined) and a reverse adaptor primer, and subsequently purified by agarose gel electrophoresis, ligated into a TA cloning vector (TOPO-TA cloning kit, Life Technologies) and sequenced.

RESULTS

Analysis of small HIV-1 RNAs bound by AGO2/RISC

In this study, we analyse miRNA production by wt HIV-1 and by the doxycycline (dox)-dependent HIV-rtTA variant (Figure 1A). In HIV-1, binding of the viral Tat protein to the TAR RNA hairpin at the 5′ end of nascent transcripts activates processive transcription from the LTR promoter and allows production of full-length viral RNAs. In HIV-rtTA, this Tat-TAR transcription activation mechanism is functionally replaced by the dox-inducible Tet-On system (46,47). For this, (i) the Tat-TAR mechanism was inactivated through mutations in the TAR bulge and loop sequences that prevent Tat binding and trans-activation of transcription (TAR^{mut}; Figure 1B), (ii) the gene encoding the dox-dependent transcriptional activator protein rtTA was inserted at the site of the accessory nef gene that is not required for gene expression and virus replication in T cell lines and (iii) tet operator (tetO) sites to which the rtTA-dox complex can bind are inserted in the viral LTR promoter. Only in the presence of dox, rtTA will bind to the tetO-LTR promoter and activate processive transcription, which will result in the production of full-length RNAs. Because HIV-rtTA does not require the Tat-TAR mechanism for the activation of transcription, this virus allows deletion of TAR without blocking viral gene expression (36).

To characterize AGO2-binding HIV-encoded small RNAs, 293T cells were transfected with plasmids expressing FLAG-tagged AGO2 (40) and either the wt HIV-1 or HIV-rtTA proviral DNA genome. HIV-rtTA transfected cells were cultured with dox to activate viral gene expression. As a control, the pBluescript vector was co-transfected instead of an HIV plasmid. 293T cells are efficiently transfected and support a high level of virus production. These cells do not express the CD4 receptor needed for HIV-1 entry, which prevents re-infection and subsequent rounds of virus replication. Two days after transfection, AGO2-bound RNAs were isolated by immune precipitation. Small RNAs (∼15–55 nt) were purified and analysed by SOLiD deep sequencing (Figure 1C). To identify the virus-derived reads, the data set was first filtered for sequences from cellular sources (Table 1). Non-viral reads that were also observed for pBluescript-transfected control cells were subsequently removed.

Table 1. SOLiD deep sequencing analysis of AGO2-bound RNAs in HIV-1 and HIV-rtTA expressing cells

Origin	Category	HIV-1	HIV-rtTA
Viral	TAR	13 945	57 721
	Other	11 654	5 051
Cellular	miRNA	33 678	18 866
	tRNA	16 671	4 572
	5S rRNA	792	256
	hY scRNA	1 499	531
	U snRNA	96	50
	LINE/SINE	76	26
	Other	658 774	188 347
Total		737 185	275 420

Analysis of 18×10^6 and 50×10^6 reads obtained for the HIV-1 and HIV-rtTA samples, respectively, with LifeScope Genomic Analysis Software using the small RNA pipeline and the highest quality value, allowing no mismatches, resulted in the mapping of 737 185 and 275 420 unambiguous reads. The number of reads with a viral or cellular origin is shown.

Approximately 3.5% (25 599 of 737 185) and 22.8% (62 772 of 275 420) of the mapped sequence reads corresponded to the HIV-1 and HIV-rtTA genome, respectively (Table 1). Alignment of these reads to the viral reference sequences revealed a prominent peak in the TAR region (Figure 2A and B). Whereas 54% of the HIV-1 reads (13 945 of 25 599 reads) corresponded to the TAR region, a significant larger number of TAR reads, 92%, were observed for HIV-rtTA (57 721 of 62 772 reads) (Table 1). Some other small peaks were observed in both alignments, but these peaks were much smaller than the peak in the TAR region. These reads did not correspond to a structured RNA region nor to any of the previously suggested HIV-1 miRNAs (17,48) and were not further investigated.

Nearly all TAR reads corresponded to the 3′ half of the TAR region (Figure 2C). Analysis of the size distribution of these TAR reads demonstrated that their size varied slightly, with a major peak at 21 nt, which is in agreement with the general miRNA size (Figure 2D) (1,49). These results indicate that the 3′ side of TAR is processed into a miRNA-like molecule that is loaded into AGO2/RISC. We further refer to this small RNA as miR-TAR-3p. No reads were observed corresponding to the 5′ side of the TAR stem in the HIV-1 and HIV-rtTA samples.

Alignment of all TAR reads demonstrates that not a unique miR-TAR-3p species is produced, but rather a small RNA population with slightly variable 5′ and 3′ ends (Figure 2E). A similar heterogeneity in length is frequently ob-

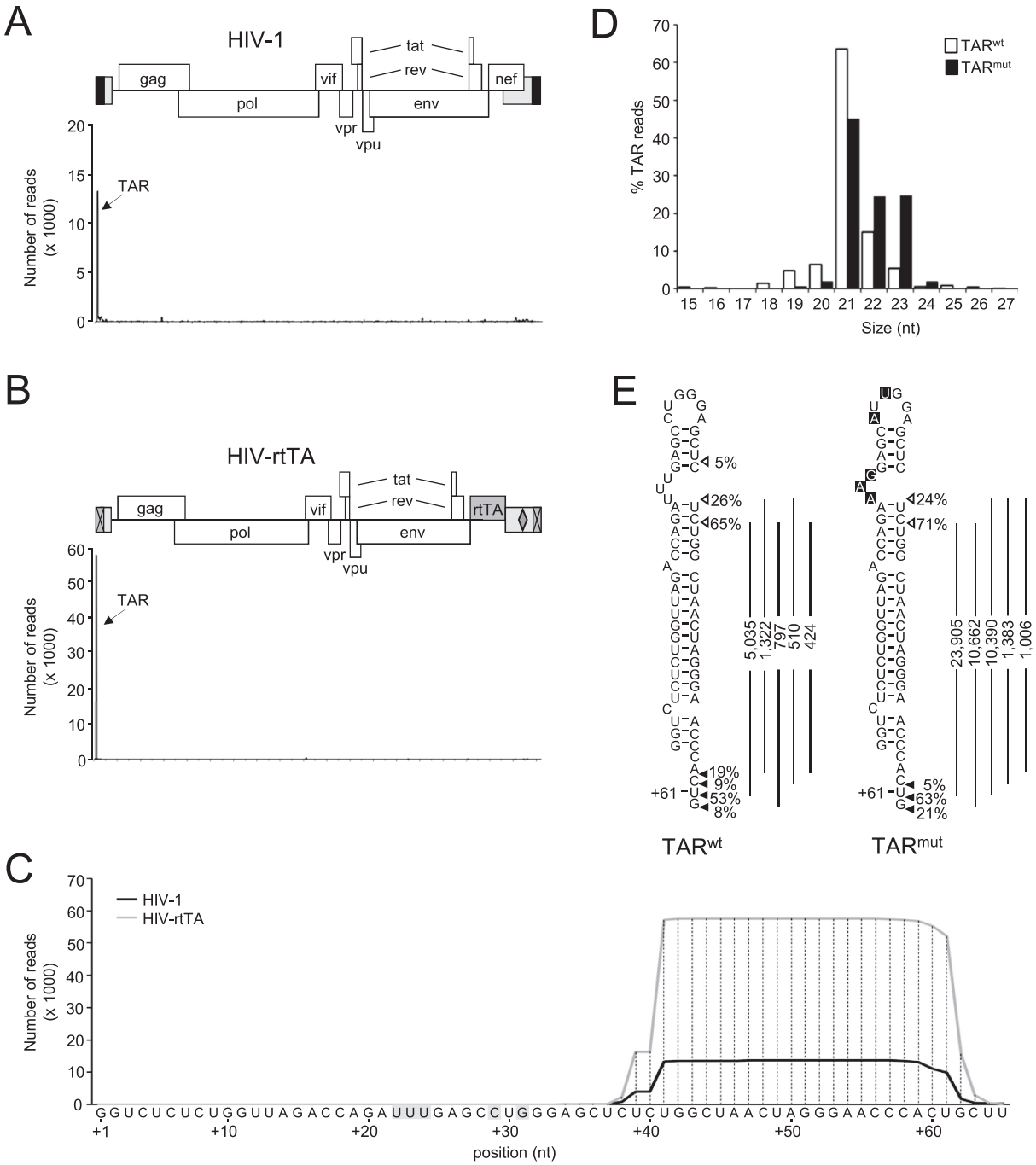

Figure 2. Deep sequencing analysis of small AGO2-bound HIV RNAs. (**A–B**) AGO2-bound RNAs isolated from 293T cells expressing HIV-1 (A) or HIV-rtTA (B) and FLAG-tagged AGO2 were analysed by SOLiD deep sequencing. The virus-encoded reads were aligned with the HIV-1 (A) and HIV-rtTA (B) RNA genome. The number of reads per nucleotide is shown. The reads corresponding to the repeat (R) region (including TAR) are shown at their 5′ position. (**C**) Alignment of the HIV-1 and HIV-rtTA derived RNAs to the TAR sequence. The wt sequence is shown with the bulge and loop nucleotides mutated in TAR^{mut} boxed in grey. (**D**) The size distribution of the TAR-derived reads is shown for the HIV-1 (TAR^{wt}) and HIV-rtTA (TAR^{mut}) samples. The total number of TAR reads (13 945 TAR^{wt} reads; 57 721 TAR^{mut} reads) was set at 100% for each sample and the percentage of reads is shown for the 15–27 nt size window. (**E**) The TAR^{wt} and TAR^{mut} structure is shown with the position of the prevailing 5′ (open arrowhead) and 3′ (closed arrowhead) ends of the TAR-derived reads indicated. The percentage of TAR-derived reads that start or end at the indicated position is shown (cut off set at 5%). The vertical lines indicate the five most frequent miR-TAR-3p RNAs with their frequency.

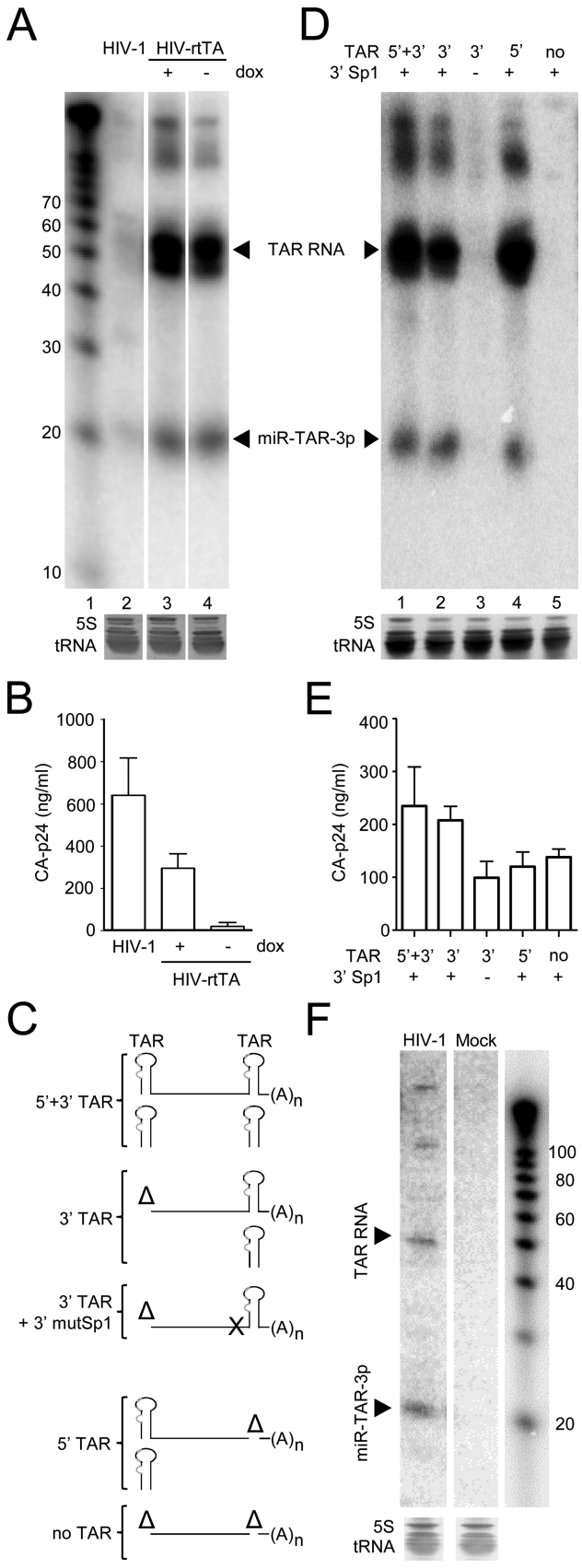

Figure 3. TAR and miR-TAR-3p RNAs are produced by non-processive transcription. (**A–B**) 293T cells were transfected with the HIV-1 and HIV-rtTA constructs and cultured for 48 h without dox (HIV-1 and HIV-rtTA) or with dox (HIV-rtTA). (**A**) Intracellular small RNAs were isolated and analysed by northern blotting. An LNA probe complementary to the miR-TAR-3p sequence was used to identify the position of miR-TAR-3p and TAR RNAs. The position of the size markers is shown on the left. Ethidium bromide staining of small 5S rRNA (5S) and tRNAs is shown as loading control below the blot. (**B**) The CA-p24 level in the culture supernatant was measured to quantify gene expression. The mean ±SD for three experiments is shown. (**C**) Expected TAR-containing transcripts produced by the HIV-rtTA variants with the TAR^{mut} element in both the 5′ and 3′LTR, only the 5′ or 3′ LTR, or no TAR element (Δ, TAR deletion). In the 3′TAR+3′mutSp1 variant, the TAR element in the 5′ LTR was deleted and the Sp1 binding sequences in the 3′ LTR region were mutated. This set of variants is based on the HIV-rtTA-Tat^{Y26A} variant (47) and all constructs carry the Tat^{Y26A} mutation (in addition to the TAR^{mut} mutations) to disable the Tat-TAR transcription activation mechanism.(**D**) 293T cells were transfected with the HIV-rtTA constructs shown in panel C and cultured for 48 h with dox. Small RNAs were isolated and analysed by northern blotting using the miR-TAR-3p probe, as described for panel A. (**E**) CA-p24 production was analysed as described for panel B. The mean ±SD for three experiments is shown. (**F**) CD4-enriched human PBMC were infected with 293T-produced wt HIV-1 virus and cultured for 48 h. Small RNAs were isolated and northern blot analysis was performed as described for Figure 3A. Mock, control uninfected PBMC. The RNA size marker is shown at the right (a short phosphorimager exposure is shown for this lane because of the high radio activity of the ^{32}P-labeled marker fragments).

served for cellular miRNAs (50). Most of the miR-TAR-3p reads started at U^{+41} (65% and 71% of the HIV-1 and HIV-rtTA TAR reads, respectively) and ended at U^{+61} (53% and 63%, respectively). The most abundant miR-TAR-3p started and ended at these dominant positions (Figure 2E). This RNA is 21 nt in size and represented 36% of all HIV-1 TAR reads and 41% of all HIV-rtTA TAR reads. The identical pattern observed for HIV-1 (with a wt TAR element) and HIV-rtTA (with a mutated TAR element) indicates that mutations in the TAR bulge and loop sequences do not affect the 5′ and 3′ ends of miR-TAR-3p.

TAR and miR-TAR-3p RNAs are produced upon non-processive transcription

Northern blot analysis of small RNAs confirmed the higher abundance of miR-TAR-3p in HIV-rtTA expressing versus wt HIV-1 expressing 293T cells (Figure 3A; compare lanes 2 and 3). In addition, larger RNA fragments of ∼60 nt were detected that correspond to the previously reported short TAR RNAs resulting from non-processive transcription starting at the LTR promoter (28,30,51). Notably, the level of these TAR RNAs is much higher for the HIV-rtTA sample, which correlates with the increased level of miR-TAR-3p RNAs and may suggest that the TAR RNAs are the precursor for miR-TAR-3p. The wt HIV-1 produced more capsid protein (CA-p24) than the dox-activated HIV-rtTA (Figure 3B). This Gag-derived protein is translated from the full-length viral RNA and the CA-p24 level thus reflects the level of processive transcription. These results suggest that the level of processive transcription was higher for wt HIV-1 (resulting in a higher CA-p24 level), whereas the level of non-processive transcription was higher for dox-activated HIV-rtTA (higher TAR RNA level). We also analysed the capacity of HIV-rtTA to produce TAR RNA and miR-TAR-3p in 293T cells in the absence of dox. HIV-rtTA produced a very low CA-p24 level without dox, which is

in agreement with the dox-control of viral processive transcription and full-length RNA production (Figure 3B). Production of the short TAR and miR-TAR-3p RNAs did however not depend on dox administration (Figure 3A; compare lanes 3 and 4), which confirms that non-processive transcription is sufficient for the production of the TAR RNAs and miR-TAR-3p.

TAR is present at both the 5′ and 3′ end of the full-length HIV-1 and HIV-rtTA transcripts (Figure 1A). To exclude the possibility that the TAR and miR-TAR-3p RNAs are produced from the TAR region at the 3′ end of full length RNAs, we analysed the small RNAs produced by HIV-rtTA variants with only the 5′ TAR, only the 3′ TAR or no TAR element (Figure 3C). As expected, deletion of both TAR elements abolished TAR and miR-TAR-3p RNA production (Figure 3D; lane 5). Deletion of the 3′ TAR did not affect TAR and miR-TAR-3p production (lane 4), which is in agreement with their 5′ TAR origin. Surprisingly, deletion of the 5′ TAR element did also not significantly reduce TAR and miR-TAR-3p RNA production (lane 2). Because transcriptional promoter activity of the 3′ LTR region may also result in the production of short TAR transcripts, we constructed an HIV-rtTA-3′TAR+3′mutSp1 variant in which the binding sites for the Sp1 transcription factor in the 3′ LTR were mutated (Figure 3C). These Sp1 mutations completely inactivate 3′ LTR promoter activity (Supplementary Figure S1). As a result, TAR sequences can only be transcribed as 3′ portion of extended HIV-rtTA-3′TAR+3′mutSp1 transcripts that initiate at the 5′ LTR and not as short TAR transcripts that initiate at the 3′ LTR. In contrast to the 3′TAR construct, this 3′TAR+3′mutSp1 variant did not produce TAR and miR-TAR-3p RNAs (Figure 3D; compare lanes 2 and 3). These results demonstrate that not only the 5′ LTR but also the 3′ LTR in the HIV-rtTA plasmid is transcriptionally active and both LTR regions drive the production of short TAR transcripts. Surprisingly, deletion of either the 5′ or 3′ TAR element did not halve the observed TAR RNA level, but this was not further investigated. In agreement with previous observations (36), deletion of the 5′ TAR element did not reduce viral CA-p24 production (Figure 3E) and deletion of the 3′ TAR element or mutation of the 3′ Sp1 sites reduced the CA-p24 level only ∼2-fold, which demonstrates that these mutations do not block full-length RNA production. Taken together, these results indicate that the TAR and miR-TAR-3p RNAs cannot be produced from the 3′ TAR region present in the full-length transcripts that are produced upon processive transcription initiating at the 5′ LTR promoter, but are exclusively derived from short transcripts resulting from non-processive transcription.

Northern blot analysis of the small RNAs isolated from CD4-enriched peripheral blood mononuclear cells (PBMC) infected with wt HIV-1 confirmed the production of the TAR precursor and miR-TAR-3p during virus replication in primary human $CD4^+$ T cells (Figure 3F).

Tat is required for miR-TAR-3p production

The experiments with dox-controlled HIV-rtTA variants demonstrated that non-processive transcription from the LTR promoter results in production of short TAR RNAs and miR-TAR-3p. The bulge and loop sequence of the TAR element in these viruses had been mutated (TAR^{mut}) to prevent Tat binding. Because these mutations may influence TAR and miR-TAR-3p production, we next tested whether non-processive transcription from the wt HIV-1 LTR promoter, with a wt TAR sequence (TAR^{wt}), is also sufficient for production of both RNA species. For this, we analysed TAR and miR-TAR-3p production of a Tat-negative HIV-1 variant (HIV-Tat^{stop}) that was constructed by introducing two translation stop codons in the Tat open reading frame (35). As expected, HIV-Tat^{stop} gene expression is low and we measured a reduced level of CA-p24 production upon transfection of the construct in 293T cells (Figure 4A). The level of transcription and CA-p24 production could be restored by addition of Tat in trans through co-transfection of a Tat-expressing plasmid (pTat). Northern blot analysis of the intracellular small RNAs revealed an increase in TAR RNA upon Tat inactivation, but no miR-TAR-3p was detectable (Figure 4B; lane 2). Trans-complementation with Tat reduced TAR RNA and increased miR-TAR-3p production to the wt levels. These results demonstrate that the TAR RNAs are produced by Tat-independent, non-processive transcription from the HIV-1 LTR promoter. Furthermore, these data indicate that Tat does not only activate processive transcription, which results in elongated viral RNAs and viral protein production, but also stimulates processing of the TAR^{wt} RNAs into miR-TAR-3p. However, these experiments do not exclude that these processes are coupled and that elongated transcripts are required for miR-TAR-3p production.

To demonstrate that the elongated TAR-containing transcripts produced upon processive transcription are not the precursor for the miR-TAR-3p, we next analysed TAR and miR-TAR-3p production from an HIV-rtTA variant with wt TAR sequences and inactivated Tat gene (HIV-rtTA-Tat^{stop}-TAR^{wt}). Processive transcription of this TAR^{wt}-Tat^{stop} virus can be activated by the administration of dox (via dox-rtTA/tetO axis) or Tat (via Tat-TAR axis). Without dox and Tat, transcription is non-processive and we did indeed measure a low level of CA-p24 production in transfected cells (Figure 4C). Addition of dox or Tat activated processive transcription and increased CA-p24 production, and highest CA-p24 production was measured when both dox and Tat were present (Figure 4C). Analysis of the small RNAs revealed that, without dox and Tat, this virus produced a high level of TAR RNA but no miR-TAR-3p RNA (Figure 4D; lane 1). Dox administration did not increase the miR-TAR-3p level (Figure 4D; lane 3), which demonstrates that the elongated transcripts produced upon processive transcription are not sufficient for miR-TAR-3p production. In contrast, Tat administration reduced the TAR RNA level and increased the miR-TAR-3p level (Figure 4D; lane 2). These results confirm that non-processive transcription is sufficient for the production of TAR RNA and that Tat activates processing of TAR RNA into miR-TAR-3p.

Changes in the TAR RNA structure activate processing into miR-TAR-3p

Previous studies demonstrated that the 3-nt bulge causes a bend in the α-helical structure of the TAR^{wt} RNA hair-

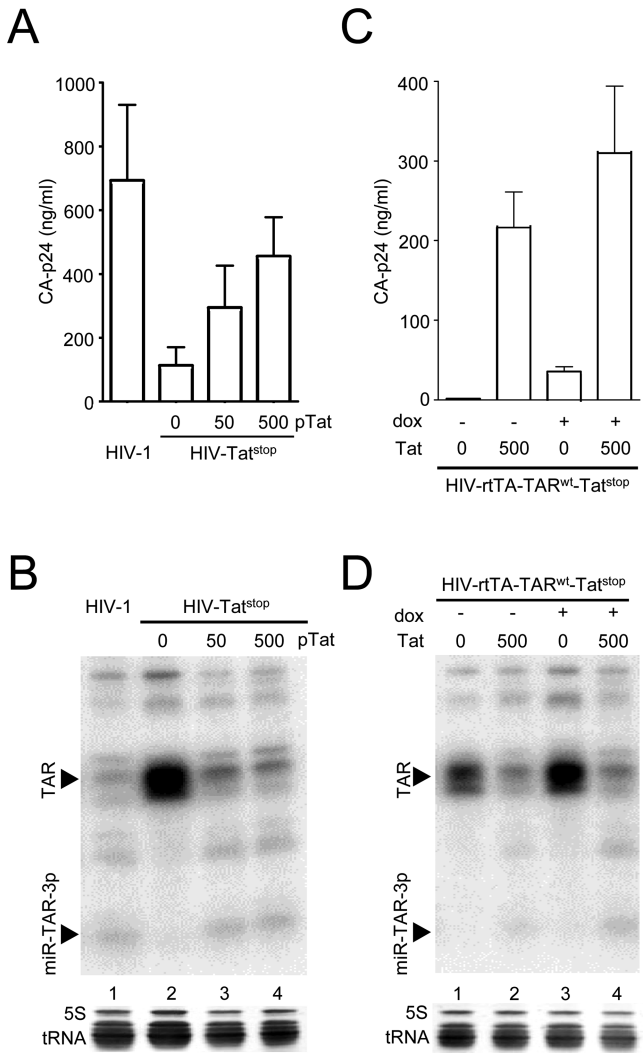

Figure 4. Tat activates miR-TAR-3p production. (**A**) 293T cells were transfected with the HIV-1 plasmid or with the Tat-deficient HIV-Tat^{stop} construct and a varying amount of Tat plasmid (0, 50 or 500 ng). The CA-p24 level in the culture supernatant was measured after 48 h. The mean ±SD for three experiments is shown. (**B**) Small RNAs were isolated and analysed by northern blotting using the miR-TAR-3p probe, as described for Figure 3A. (**C**) 293T cells were transfected with the Tat-deficient HIV-rtTA-Tat^{stop} construct with a wild-type TAR element (TAR^{wt}). When indicated, cells were co-transfected with 500 ng pTat and cultured in the presence of dox. The CA-p24 level in the culture supernatant was measured after 48 h. The mean ±SD for three experiments is shown. (**D**) Small RNAs isolated from the transfected cells were analysed by northern blotting using the miR-TAR-3p probe, as described for Figure 3A.

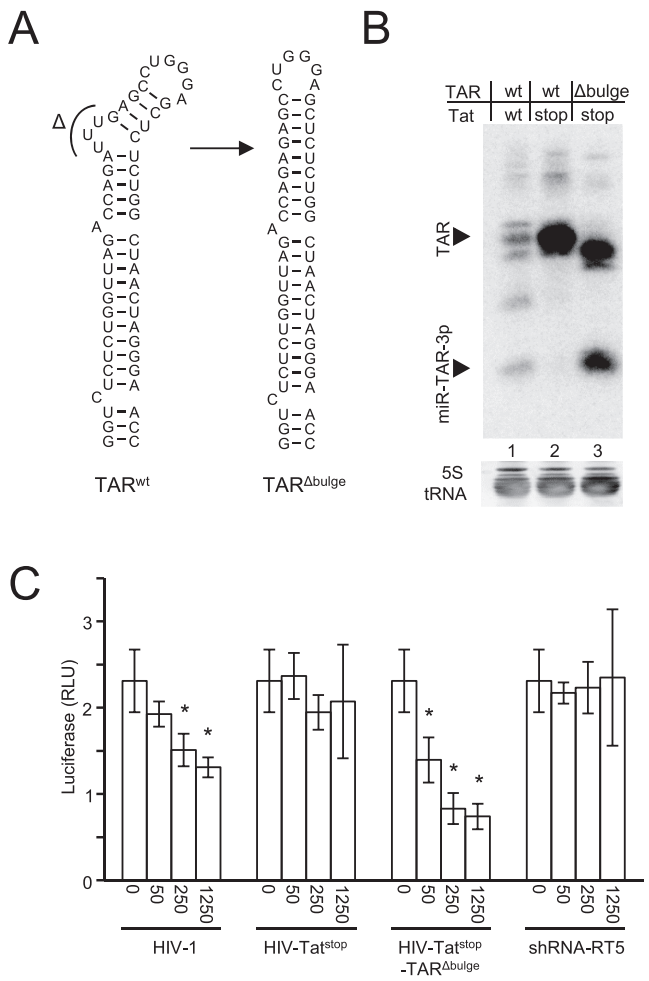

Figure 5. Bulge deletion activates TAR RNA processing. (**A**) In the HIV-1 TAR$^{\Delta bulge}$ mutant, the 3-nt TAR bulge (nt +22 to +24) was deleted. (**B**) 293T cells were transfected with wt HIV-1 and HIV-Tat^{stop} variants with either a wt or bulge-deleted TAR element (TAR^{wt} and TAR$^{\Delta bulge}$, respectively). Small RNAs were isolated after 48 h and analysed by northern blot blotting using the miR-TAR-3p probe as described for Figure 3A. (**C**) A luciferase reporter construct containing the miR-TAR-3p target sequence in the 3′ UTR was transfected into 293T cells together with 0–1250 ng HIV-1, HIV-Tat^{stop}, HIV-Tat^{stop}-TAR$^{\Delta bulge}$ or a plasmid expressing a non-related shRNA-RT5 (42). Luciferase production was measured 48 h after transfection. The mean values ±SD for four experiments is shown. Statistical analysis using independent samples T-test analysis was used to compare the luciferase activities obtained without and with co-transfection of the HIV-1 or shRNA-RT5 constructs (*, $P < 0.01$).

pin (52–54), and Tat binding was shown to trigger TAR straightening (54–56). We hypothesized that the short TAR RNAs require this Tat-induced straight conformation for processing into miRNAs. To investigate the effect of such a conformational change on TAR RNA processing, we straightened the TAR structure by deleting the 3-nt bulge in HIV-Tat^{stop} (TAR$^{\Delta bulge}$ in Figure 5A) and compared production of small TAR RNAs by the TAR^{wt} and TAR$^{\Delta bulge}$ variants (Figure 5B). Whereas HIV-Tat^{stop}-TAR^{wt} produced TAR RNA but no miR-TAR-3p (Figure 5B; lane 2), the TAR$^{\Delta bulge}$ variant demonstrated efficient TAR RNA processing, resulting in a high miR-TAR-3p level (Figure 5B; lane 3). This result indicates that the wt TAR conformation hampers its processing into miR-TAR-3p and this restriction can be lifted by deletion of the bulge nucleotides.

It should be noted that whereas the HIV-1 and HIV-rtTA variants with the wt TAR element required Tat for the processing of the TAR RNAs into miR-TAR-3p (Figure 4B and D), the HIV-rtTA variant with mutations in TAR that prevented Tat binding (TAR^{mut}) demonstrated partial processing of the TAR RNAs, both in the presence and absence of Tat (Supplementary Figure S2; Figure 3A, + and − dox: high and low production of viral proteins, including Tat, respectively). Possibly, the nucleotide substitutions

in the bulge region of TAR^{mut} affected the RNA structure and allowed partial cleavage.

The miR-TAR-3p can silence target RNAs

MiRNAs can target mRNAs with complementary sequences for cleavage or translational repression. To test the capacity of the miR-TAR-3p to knock-down gene expression, we constructed a luciferase reporter with the sequence complementary to miR-TAR-3p in the 3′ untranslated RNA region. Upon transfection of this reporter into 293T cells, a high luciferase level was measured after 48 hr (Figure 5C). This luciferase level gradually decreased when the cells were co-transfected with an increasing amount of the miR-TAR-3p expressing wt HIV-1 and HIV-Tat^{stop}-TAR$^{\Delta bulge}$ constructs. The latter was a more effective inhibitor, which is in agreement with increased miR-TAR-3p production (as demonstrated in Figure 5B). Co-transfection with the HIV-Tat^{stop} construct that does not produce miR-TAR-3p did not reduce the luciferase level. Similarly, luciferase expression was not influenced by co-transfection of a control plasmid expressing a non-related short hairpin RNA (shRNA-RT5; (42)) with no sequence homology to the miR-TAR-3p target sequence. As an additional control experiment, a luciferase reporter construct with the shRNA-RT5 target sequence in the 3′ untranslated RNA region was transfected into 293T cells together with the different HIV-1 variants and the shRNA-RT5 expressing plasmid (Supplementary Figure S3). Expression of this luciferase reporter was significantly reduced by the shRNA-RT5 plasmid but not by the miR-TAR-3p producing HIV-1 and HIV-Tat^{stop}-TAR$^{\Delta bulge}$ constructs, which demonstrates the sequence specificity of miR-TAR-3p. Taken together, these results show that miR-TAR-3p is able to knock-down the expression of target RNAs.

TAR RNA is processed by Dicer

The role of Dicer in miR-TAR-3p production was analysed in HCT-116 cells expressing either wt (Dicer^{wt}) or exon 5-disrupted Dicer (Dicer^{ex5}). This ex5 mutation in the helicase domain reduces Dicer activity (32). Unfortunately, transfection with the TAR^{wt} encoding HIV-1 plasmid or HIV-1 derived LTR construct did not yield detectable levels of miR-TAR-3p, which may be due to relatively inefficient transfection of these cells (data not shown). We therefore transfected the cells with a TAR^{mut} expressing LTR construct derived from the HIV-rtTA variant that produces significantly more TAR RNA and miR-TAR-3p (Figure 3A). Both the TAR RNA precursor and miR-TAR-3p were detected in Dicer^{wt} cells (Figure 6A). Importantly, an increased level of TAR RNA and a concomitant reduction of the miR-TAR-3p signal was observed in Dicer^{ex5} cells. Processing of TAR^{mut} into miR-TAR-3p was not influenced by Tat, which is in agreement with previous observations (as described above; Supplementary Figure S2B). Analysis of the Dicer-mediated processing of shRNAs in parallel experiments confirmed the high and low Dicer activity in these Dicer^{wt} and Dicer^{ex5} cells, respectively (57). These results indicate that Dicer is involved in the processing of the TAR RNAs.

The 3′ end of TAR RNA corresponds with the 3′ end of miR-TAR-3p

To confirm that TAR RNA—like canonical cellular pre-miRNAs—can bind to Dicer, we transfected 293T cells with the HIV-Tat^{stop} construct that produces a high level of TAR^{wt} RNA (Figure 4B) together with a plasmid expressing FLAG-tagged Dicer (43) or the non-related control FLAG-tagged HCV E2 protein. At 48 h after transfection, the Dicer and E2 bound RNAs were isolated by immunoprecipitation. The bound and unbound small RNA fractions were analysed for the presence of the TAR RNA and the cellular Let-7A pre-miRNA by reverse-transcription PCR (Figure 6B), followed by gel electrophoresis (Figure 6C). The TAR RNA and Let-7A pre-miRNA were highly enriched in the Dicer bound fraction, but not in the E2 bound fraction, which indicates that Dicer can bind TAR.

To characterize the TAR 3′ end, we cloned and sequenced the TAR cDNA fragment isolated upon RT-PCR analysis of the Dicer-bound RNA fraction (Figure 6D). We identified several TAR RNA fragments with a slightly variable 3′ end (ranging from position +59 to + 61). This 3′ end of the TAR RNA matches the 3′ end of the miR-TAR-3p (Figure 2E), which is in agreement with the precursor function of TAR RNA.

DISCUSSION

The debate about whether HIV-1 encodes miRNAs is ongoing for 10 years. The fact that miRNA production via the canonical miRNA pathway, involving subsequent microprocessor and Dicer cleavage of the primary transcript, would result in degradation of the viral RNA genome and impede HIV-1 replication was long considered a strong argument against HIV-1 encoded miRNAs. In this study we demonstrate how HIV-1 can produce a miRNA-like small RNA molecule without hampering virus replication. First, we show that HIV-1 produces a small RNA from the 3′ side of the TAR RNA hairpin. Like canonical miRNAs, this miR-TAR-3p is ∼21-nt in size, binds to AGO2 and is able to repress the expression of mRNAs bearing the complementary target sequence. Second, we demonstrate that the short TAR RNAs produced upon non-processive transcription from the HIV-1 LTR promoter function as precursor for miR-TAR-3p and are processed by Dicer. MiR-TAR-3p is thus not generated via the canonical miRNA pathway in which cleavage of the primary transcript by microprocessor is needed to release the pre-miRNA, but via a non-canonical pathway in which the RNA precursor is produced by pausing and premature termination of RNAP II transcription. By selectively using these short TAR RNAs as precursor, HIV-1 can produce miR-TAR-3p without inducing cleavage of its RNA genome. Third, we demonstrate that the viral Tat protein activates TAR processing into miR-TAR-3p.

The 21-nt miR-TAR-3p that we identified overlaps with earlier suggested 3′ TAR-derived small RNAs (17–21,26). Schopman *et al*. (20) observed the same miR-TAR-3p read upon deep-sequence analysis of HIV-rtTA expressing cells, but other studies identified small RNA molecules that differ in exact size and position (Figure 7A). We did not detect any

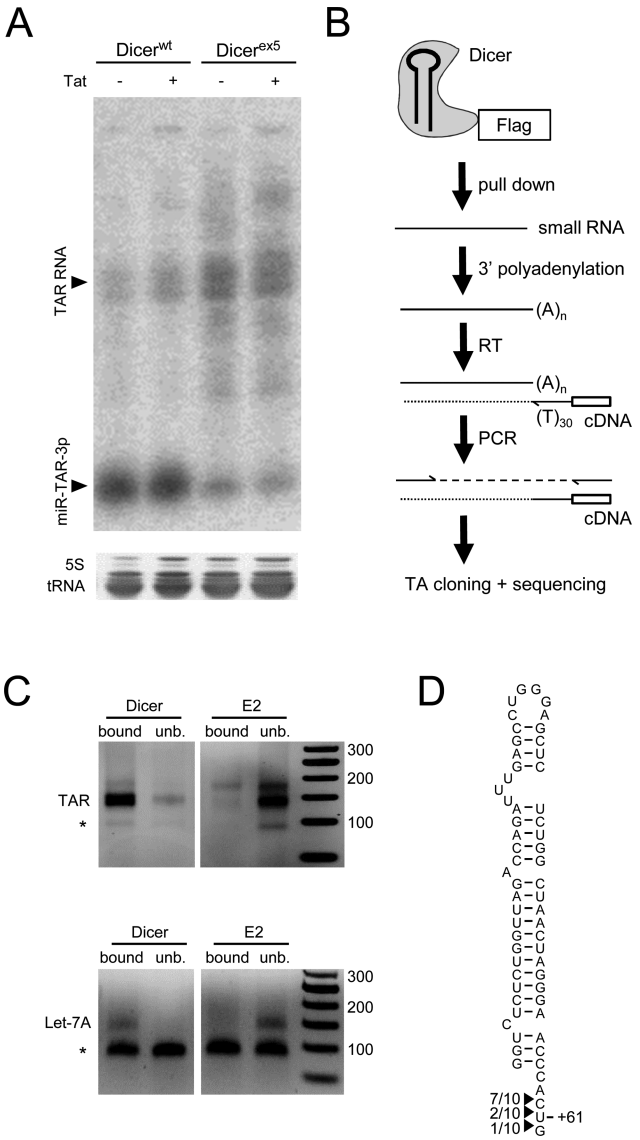

Figure 6. Dicer processes TAR RNA into miR-TAR-3p. (**A**) HCT-116 cells expressing wt or exon5-disrupted Dicer (ex5) were transfected with the plasmid pLTR-2ΔtetO-luc^{ff} (36) in which expression of TAR^{mut}-containing RNAs is driven by the HIV-rtTA U3 promoter. When indicated, cells were co-transfected with 500 ng pTat. The RNA was analysed after 48 h by northern blotting using the miR-TAR-3p probe. (**B**) Experimental design for the isolation and characterization of Dicer-bound TAR RNAs from 293T cells transfected with the plasmid expressing FLAG-tagged Dicer and the TAR^{wt}-expressing HIV-Tat^{stop} construct. (**C**) 293T cells were transfected with the HIV-Tat^{stop} construct together with a plasmid expressing FLAG-tagged Dicer (left panels) or FLAG-tagged HCV E2 (right panels). Dicer and E2 bound RNAs were isolated by immunoprecipitation. The TAR RNA (upper panels) and Let-7A pre-miRNA (lower panels) in the bound and unbound small RNA fractions were detected by RT-PCR and gel electrophoresis. The position of the TAR RNA and Let-7A pre-miRNA RT-PCR product is indicated. *, RT-PCR product with only primer and adaptor sequences, lacking any insert sequence. (**D**) The RT-PCR product corresponding to the TAR RNA in the Dicer bound fraction was TA-cloned and 10 DNA fragments were sequenced to determine the 3′ end of the TAR RNA. The position (indicated with arrowhead) and frequency of the identified 3′ ends are shown.

other previously suggested HIV-1 miRNA (17,48). The differences between our and previous results are likely due to technical differences. The earlier studies used in silico analysis (17) or traditional cloning and sequencing (18), RNase protection (19) or deep sequencing (20,21,26) of total intracellular RNA pools. We combined AGO2-pull down with deep sequencing to specifically analyse small RNA molecules that are loaded into the AGO2/RISC complex. This method resulted in a large number of TAR-derived viral reads for HIV-1 and HIV-rtTA expressing 293T cells (13 945 and 57 721 reads, respectively) that was comparable to the number obtained for cellular miRNAs (33 678 and 18 866, respectively; Table 1). The size of the AGO2-captured viral RNA reads peaked at 21 nt (Figure 2D and data not shown), which is in accordance with the expected size for miRNAs. In the previous sequencing studies that analysed the total small RNA pool, the size of the HIV-1 reads peaked at 18 nt or less (20,26). Possibly, these numerous small RNA reads interfered with the detection of miR-TAR-3p. We observed some heterogeneity in the 5′ and 3′ end of the miR-TAR-3p reads in the sequencing analysis. Such heterogeneity is more frequently observed for cellular and viral miRNAs in deep sequencing analyses (58–60). In the northern blot analysis, a discrete size of 21-nt was observed for miR-TAR-3p.

Whisnant *et al*. detected TAR-derived RNAs when deep sequencing total intracellular small RNA pools in different HIV-1 infected cells (Figure 7A), but did not identify miR-TAR-3p when analyzing the protein–RNA complexes pulled-down from HIV-1 infected TZM-bl cells by immunoprecipitation using an antibody recognizing AGO1, AGO2 and AGO3 (26). Remarkably, when using a crosslinking-immunoprecipitation technique (PAR-CLIP) to analyse the AGO-bound RNAs in HIV-1 infected C8166 and TZM-bl cells, these authors detected a cluster of small RNAs in the TAR region (∼1000 and ∼2600 reads in C8166 and TZM-bl cells, respectively; Figure 5 in (26)), but these RNAs were not discussed. Importantly, we detected miR-TAR-3p not only in our AGO2-pull down/deep sequencing analysis, but also demonstrate that this small RNA can knock down expression of target-containing mRNAs (Figure 5C), which confirms its association with the AGO2/RISC complex. Moreover, we confirmed the production of this miR-TAR-3p and its TAR precursor in HIV-1 expressing 293T cells (Figures 3A, 4B, 5B) and HIV-1 infected primary T cells (Figure 3F) by northern blot analysis of the intracellular small RNA pool.

We demonstrate that Dicer can bind TAR RNA and that a decrease of the intracellular Dicer activity reduces TAR processing into miR-TAR-3p. These results indicate that Dicer cleaves the TAR precursor. The viral Tat protein was found to stimulate processing of TAR RNA into miR-TAR-3p. Thus, Tat not only activates processive transcription from the LTR promoter but also triggers processing of the TAR RNAs that are formed during non-processive transcription. The observed simultaneous production of full-length HIV-1 RNAs (reflected by the CA-p24 level; Figure 4A) and miR-TAR-3p (Figure 4B) upon Tat induction indicates that activation of processive transcription does not switch off non-processive transcription.

A

B

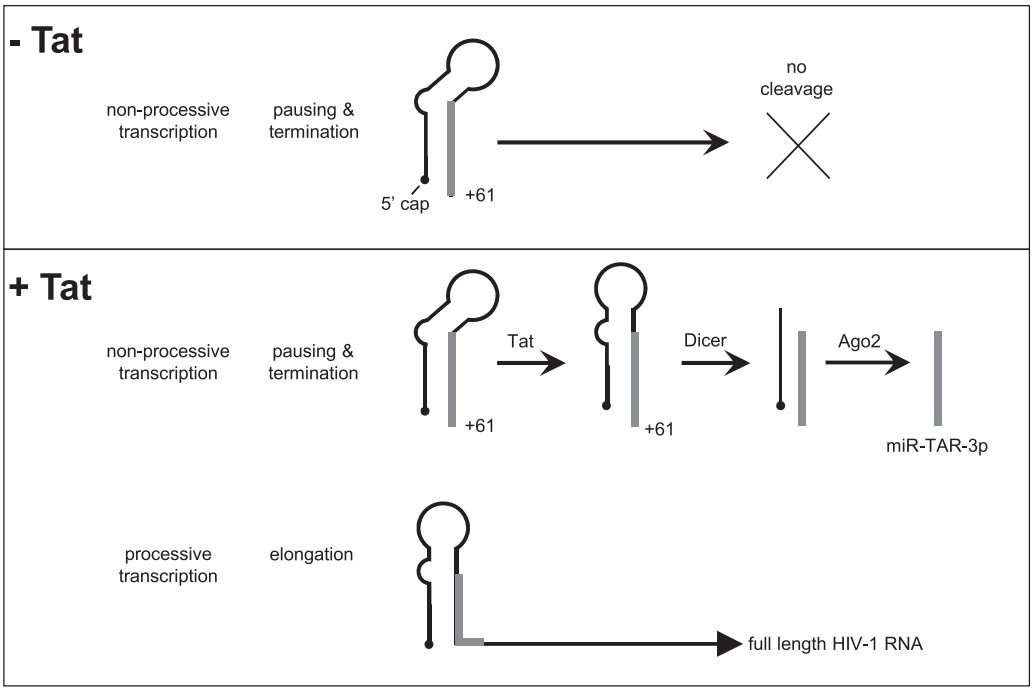

Figure 7. Production of the TAR-encoded miRNA-like small RNA. (**A**) Alignment of the TAR-derived small RNAs identified in different studies. All studies (except the in silico analysis) characterized the TAR RNAs in HIV-1 expressing cells, but different techniques were used: a–b, SOLiD deep sequencing of AGO2-bound HIV-1 (a) and HIV-rtTA RNAs (b; this study); c, Illumina deep sequencing of HIV-1 RNAs (26); d–f, SOLiD deep sequencing of small HIV-1 (d: ref 21; e: 20) and HIV-rtTA RNAs (f: 20); g, RNAse protection analysis (RPA) of HIV-1 RNAs (19); h, cloning and sequencing of small HIV-1 RNAs (18,22); i, in silico analysis (17). In the upper line the HIV-1 LTR sequence is shown with the TAR region (+1 to +57) boxed in grey and the transcription start site indicated (+1). The dominant 5p and 3p sequence found in each study is shown with the number of reads or clones indicated at the right. (**B**) Model for HIV-1 TAR RNA and miR-TAR-3p production based on our and previous findings discussed in the text. In the absence of Tat, non-processive RNAP II complexes are formed at the LTR promoter and transcription is initiated but frequently pauses when TAR is formed. Subsequent premature termination of transcription results in the production of short 5′ capped TAR RNAs. These TAR RNAs are not further processed. Possibly, the bended structure of the TAR RNAs prevents Dicer cleavage. In the presence of Tat, binding of Tat to TAR causes straightening of the hairpin structure, which may allow Dicer cleavage. As discussed in the text, alternative scenarios are possible for this Tat-activation of TAR processing. Cleavage of TAR by Dicer results in the production of miR-TAR-5p and miR-TAR-3p. MiR-TAR-3p is loaded onto the AGO2/RISC complex, whereas loading of miR-TAR-5p is blocked by the 5′cap. Binding of Tat to TAR also recruits the pTEFb complex to the LTR promoter, which results in phosphorylation of the RNAP II complex and activation of processive transcription. Because the TAR stem in the extended transcripts is too short for efficient microprocessor cleavage, full-length RNAs can be produced and virus replication will be allowed.

Interestingly, we observed that whereas wt TAR RNA was processed exclusively in the presence of Tat, the mutated and bulge-deleted TAR RNAs were processed in the absence of Tat. Possibly, TAR processing is controlled by the hairpin structure and Tat-binding results in a cleavage-prone conformation. In this scenario, the bend in the α-helical stem structure caused by the wt 3-nt bulge (52–54) may hinder Dicer cleavage. Binding of Tat to the TAR bulge is known to straighten the hairpin (54–56), which may result in a cleavage-prone RNA conformation. Mutation or deletion of the bulge nucleotides may similarly affect TAR RNA bending and processing. However, alternative scenarios are possible for how Tat affects TAR processing. For example, the 3-nt TAR bulge may bind a protein factor that

prevents Dicer cleavage. Tat binding may displace this inhibitory factor and activate Dicer processing. In this scenario, bulge deletion or mutation may prevent binding of the inhibitory factor and activate processing. Alternatively, Tat may have an indirect effect by influencing the production of a—yet unidentified—cellular factor that stimulates processing of wt TAR. This scenario seems less likely, as it does not explain how bulge deletion or mutation activates TAR processing in the absence of Tat, unless these TAR modifications result in a cleavage-prone RNA conformation that does not require the cellular factor for processing.

It has been shown that microprocessor binds nascent TAR-containing transcripts at the HIV-1 transcription start site and influences RNAP II transcription elongation (21). Microprocessor may similarly bind to cellular nascent RNA transcripts and regulate transcription of cellular genes (21,61,62). Gromak *et al*. demonstrated that this microprocessor function does not depend on the RNA cleavage activity of Drosha (61). It seems likely that microprocessor cleavage is also not involved in TAR RNA and miR-TAR-3p production. First, TAR RNA may not be a good substrate because the TAR stem consists of only 23 bp, whereas microprocessor requires extended duplexes of ∼33 bp for efficient binding and cleavage (4,26). Furthermore, microprocessor normally cleaves a pri-miRNA stem at ∼11 bp from its base and the 3′ end of miR-TAR-3p does not correspond with this position in the TAR hairpin. We demonstrate that TAR RNAs that are produced by non-processive transcription function as miR-TAR-3p precursor. The 3′ end of miR-TAR-3p does correspond with the strong RNAP II transcription pause site that was previously identified in *in vitro* HIV-1 transcription assays (28) and with the 3′ end of short HIV-1 transcripts produced during non-processive transcription in HIV-Tat^{stop} transfected 293T cells (Figure 6D) and latently infected U1 cells, which harbour two HIV-1 copies with defective Tat genes (51). Taken together, these results indicate that the 3′ end of TAR and miR-TAR-3p is created by pausing and subsequent premature termination of transcription.

Cellular promoter-proximal transcripts resulting from RNAP II pausing and subsequent premature transcription termination that fold a hairpin RNA structure can function as miRNA precursor (62,63). Xie *et al*. (63) demonstrated that after Dicer cleavage of such capped pre-miRNAs, the capped 5p strand is excluded from loading onto AGO2 and only the 3p strand is efficiently loaded. The 5′ end of HIV-1 transcripts is also capped (64,65), which may explain why we did not detect small RNAs corresponding to the 5′ side of the TAR stem in the AGO2-bound RNA fraction. Production and processing of the TAR RNA may thus be very similar to that of these cellular pre-miRNAs. The model summarizing how HIV-1 produces miR-TAR-3p is presented in Figure 7B.

The retroviruses BLV (13,14), BFV (15), SFV (16) and ALV-J (11) were previously shown to produce small RNAs that may function as miRNA. In these studies, deep sequencing analysis of the total intracellular small RNA pool of virus-infected cells demonstrated high abundance of the miRNAs. As discussed above, several studies in which the total small RNA pool of HIV-1 infected cells was similarly analysed failed to detect miR-TAR-3p. However, we observed miR-TAR-3p at a similar level as cellular miRNAs when sequencing AGO2-captured small RNAs. Assuming that the TAR-derived small RNAs are not preferentially detected, our results thus suggest that miR-TAR-3p is produced at a similar level as cellular miRNAs.

We demonstrate that HIV-1 does not use the canonical miRNA pathway for miR-TAR-3p production, but selectively uses the short TAR RNA transcripts resulting from non-processive RNAP II transcription as the precursor. ALV-J also uses an RNAP II transcript as precursor for the miRNA, but this miRNA is processed via the canonical miRNA pathway, involving successive cleavage of the pri-miRNA transcript by Drosha and Dicer (11). Like HIV-1, BLV, BFV and SFV use a non-canonical pathway for the production of small RNAs (13–16). These viruses produce short sub-genomic RNAP III transcripts that function as miRNA precursor, whereas the extended RNAP II transcripts that also contain the miRNA sequence are not processed (as demonstrated for BLV (13) and SFV (16) and predicted for BFV (15)). The production of designated transcripts that function as precursor thus seems a general retroviral strategy to produce these virus-encoded small RNAs without interfering with genomic and mRNA production.

SUPPLEMENTARY DATA

Supplementary Data are available at NAR Online.

ACKNOWLEDGEMENTS

We thank Ted Bradley for his help in the SOLiD deep sequencing and Stephan Heynen for performing CA-p24 ELISA.

FUNDING

Netherlands Organisation for Scientific Research (Chemical Sciences Division; NWO-CW; Top grant). Funding for open access charge: Netherlands Organisation for Scientific Research (NWO; Incentive Fund Open Access).
Conflict of interest statement. None declared.

REFERENCES

1. Bartel,D.P. (2004) MicroRNAs: genomics, biogenesis, mechanism, and function. *Cell*, **116**, 281–297.
2. Lee,Y., Ahn,C., Han,J., Choi,H., Kim,J., Yim,J., Lee,J., Provost,P., Radmark,O., Kim,S. *et al.* (2003) The nuclear RNase III Drosha initiates microRNA processing. *Nature*, **425**, 415–419.
3. Shiohama,A., Sasaki,T., Noda,S., Minoshima,S. and Shimizu,N. (2003) Molecular cloning and expression analysis of a novel gene DGCR8 located in the DiGeorge syndrome chromosomal region. *Biochem. Biophys. Res. Commun.*, **304**, 184–190.
4. Han,J., Lee,Y., Yeom,K.H., Nam,J.W., Heo,I., Rhee,J.K., Sohn,S.Y., Cho,Y., Zhang,B.T. and Kim,V.N. (2006) Molecular basis for the recognition of primary microRNAs by the Drosha-DGCR8 complex. *Cell*, **125**, 887–901.
5. Provost,P., Dishart,D., Doucet,J., Frendewey,D., Samuelsson,B. and Radmark,O. (2002) Ribonuclease activity and RNA binding of recombinant human Dicer. *EMBO J.*, **21**, 5864–5874.
6. Zhang,H., Kolb,F.A., Brondani,V., Billy,E. and Filipowicz,W. (2002) Human Dicer preferentially cleaves dsRNAs at their termini without a requirement for ATP. *EMBO J.*, **21**, 5875–5885.
7. Kim,V.N. (2005) MicroRNA biogenesis: coordinated cropping and dicing. *Nat. Rev. Mol. Cell Biol.*, **6**, 376–385.

8. Schwarz,D.S., Hutvagner,G., Du,T., Xu,Z., Aronin,N. and Zamore,P.D. (2003) Asymmetry in the assembly of the RNAi enzyme complex. *Cell*, **115**, 199–208.
9. Khvorova,A., Reynolds,A. and Jayasena,S.D. (2003) Functional siRNAs and miRNAs exhibit strand bias. *Cell*, **115**, 209–216.
10. Kincaid,R.P. and Sullivan,C.S. (2012) Virus-encoded microRNAs: an overview and a look to the future. *PLoS Pathogens*, **8**, e1003018.
11. Yao,Y., Smith,L.P., Nair,V. and Watson,M. (2014) An avian retrovirus uses canonical expression and processing mechanisms to generate viral microRNA. *J. Virol.*, **88**, 2–9.
12. Harwig,A., Das,A.T. and Berkhout,B. (2014) Retroviral microRNAs. *Curr. Opin. Virol.*, **7**, 47–54.
13. Kincaid,R.P., Burke,J.M. and Sullivan,C.S. (2012) RNA virus microRNA that mimics a B-cell oncomiR. *Proc. Natl. Acad. Sci. U.S.A.*, **109**, 3077–3082.
14. Rosewick,N., Momont,M., Durkin,K., Takeda,H., Caiment,F., Cleuter,Y., Vernin,C., Mortreux,F., Wattel,E., Burny,A. *et al.* (2013) Deep sequencing reveals abundant noncanonical retroviral microRNAs in B-cell leukemia/lymphoma. *Proc. Natl. Acad. Sci. U.S.A.*, **110**, 2306–2311.
15. Whisnant,A.W., Kehl,T., Bao,Q., Materniak,M., Kuzmak,J., Lochelt,M. and Cullen,B.R. (2014) Identification of novel, highly expressed retroviral microRNAs in cells infected by bovine foamy virus. *J. Virol.*, **88**, 4679–4686.
16. Kincaid,R.P., Chen,Y., Cox,J.E., Rethwilm,A. and Sullivan,C.S. (2014) Noncanonical microRNA (miRNA) biogenesis gives rise to retroviral mimics of lymphoproliferative and immunosuppressive host miRNAs. *mBio*, **5**, e00074.
17. Bennasser,Y., Le,S.Y., Yeung,M.L. and Jeang,K.T. (2004) HIV-1 encoded candidate micro-RNAs and their cellular targets. *Retrovirology*, **1**, 43.
18. Klase,Z., Kale,P., Winograd,R., Gupta,M.V., Heydarian,M., Berro,R., McCaffrey,T. and Kashanchi,F. (2007) HIV-1 TAR element is processed by Dicer to yield a viral micro-RNA involved in chromatin remodeling of the viral LTR. *BMC Mol. Biol.*, **8**, 63.
19. Ouellet,D.L., Plante,I., Landry,P., Barat,C., Janelle,M.E., Flamand,L., Tremblay,M.J. and Provost,P. (2008) Identification of functional microRNAs released through asymmetrical processing of HIV-1 TAR element. *Nucleic Acids Res.*, **36**, 2353–2365.
20. Schopman,N.C., Willemsen,M., Liu,Y.P., Bradley,T., van Kampen,A., Baas,F., Berkhout,B. and Haasnoot,J. (2012) Deep sequencing of virus-infected cells reveals HIV-encoded small RNAs. *Nucleic Acids Res.*, **40**, 414–427.
21. Wagschal,A., Rousset,E., Basavarajaiah,P., Contreras,X., Harwig,A., Laurent-Chabalier,S., Nakamura,M., Chen,X., Zhang,K., Meziane,O. *et al.* (2012) Microprocessor, Setx, Xrn2, and Rrp6 co-operate to induce premature termination of transcription by RNAPII. *Cell*, **150**, 1147–1157.
22. Klase,Z., Winograd,R., Davis,J., Carpio,L., Hildreth,R., Heydarian,M., Fu,S., McCaffrey,T., Meiri,E., Ayash-Rashkovsky,M. *et al.* (2009) HIV-1 TAR miRNA protects against apoptosis by altering cellular gene expression. *Retrovirology*, **6**, 18.
23. Ouellet,D.L., Vigneault-Edwards,J., Letourneau,K., Gobeil,L.A., Plante,I., Burnett,J.C., Rossi,J.J. and Provost,P. (2013) Regulation of host gene expression by HIV-1 TAR microRNAs. *Retrovirology*, **10**, 86.
24. Lin,J. and Cullen,B.R. (2007) Analysis of the interaction of primate retroviruses with the human RNA interference machinery. *J. Virol.*, **81**, 12218–12226.
25. Pfeffer,S., Zavolan,M., Grasser,F.A., Chien,M., Russo,J.J., Ju,J., John,B., Enright,A.J., Marks,D., Sander,C. *et al.* (2004) Identification of virus-encoded microRNAs. *Science*, **304**, 734–736.
26. Whisnant,A.W., Bogerd,H.P., Flores,O., Ho,P., Powers,J.G., Sharova,N., Stevenson,M., Chen,C.H. and Cullen,B.R. (2013) In-depth analysis of the interaction of HIV-1 with cellular microRNA biogenesis and effector mechanisms. *mBio*, **4**, e000193.
27. Berkhout,B., Silverman,R.H. and Jeang,K.T. (1989) Tat trans-activates the human immunodeficiency virus through a nascent RNA target. *Cell*, **59**, 273–282.
28. Palangat,M., Meier,T.I., Keene,R.G. and Landick,R. (1998) Transcriptional pausing at +62 of the HIV-1 nascent RNA modulates formation of the TAR RNA structure. *Mol. Cell*, **1**, 1033–1042.
29. Bres,V., Yoh,S.M. and Jones,K.A. (2008) The multi-tasking P-TEFb complex. *Curr. Opin. Cell Biol.*, **20**, 334–340.
30. Kao,S.Y., Calman,A.F., Luciw,P.A. and Peterlin,B.M. (1987) Anti-termination of transcription within the long terminal repeat of HIV-1 by tat gene product. *Nature*, **330**, 489–493.
31. Margaritis,T. and Holstege,F.C. (2008) Poised RNA polymerase II gives pause for thought. *Cell*, **133**, 581–584.
32. Cummins,J.M., He,Y., Leary,R.J., Pagliarini,R., Diaz,L.A. Jr, Sjoblom,T., Barad,O., Bentwich,Z., Szafranska,A.E., Labourier,E. *et al.* (2006) The colorectal microRNAome. *Proc. Natl. Acad. Sci. U.S.A.*, **103**, 3687–3692.
33. Jeeninga,R.E., Jan,B., van den Berg,H. and Berkhout,B. (2006) Construction of doxycyline-dependent mini-HIV-1 variants for the development of a virotherapy against leukemias. *Retrovirology*, **3**, 64.
34. Peden,K., Emerman,M. and Montagnier,L. (1991) Changes in growth properties on passage in tissue culture of viruses derived from infectious molecular clones of HIV-1LAI, HIV-1MAL, and HIV-1ELI. *Virology*, **185**, 661–672.
35. Das,A.T., Harwig,A. and Berkhout,B. (2011) The HIV-1 Tat protein has a versatile role in activating viral transcription. *J. Virol.*, **85**, 9506–9516.
36. Das,A.T., Harwig,A., Vrolijk,M.M. and Berkhout,B. (2007) The TAR hairpin of human immunodeficiency virus type 1 can be deleted when not required for Tat-mediated activation of transcription. *J. Virol.*, **81**, 7742–7748.
37. Das,A.T., Klaver,B. and Berkhout,B. (1998) The 5' and 3' TAR elements of human immunodeficiency virus exert effects at several points in the virus life cycle. *J. Virol.*, **72**, 9217–9223.
38. Das,A.T., Zhou,X., Vink,M., Klaver,B., Verhoef,K., Marzio,G. and Berkhout,B. (2004) Viral evolution as a tool to improve the tetracycline-regulated gene expression system. *J. Biol. Chem.*, **279**, 18776–18782.
39. Mikaelian,I. and Sergeant,A. (1992) A general and fast method to generate multiple site directed mutations. *Nucleic Acids Res.*, **20**, 376.
40. Kwak,P.B. and Tomari,Y. (2012) The N domain of Argonaute drives duplex unwinding during RISC assembly. *Nat. Struct. Mol. Biol.*, **19**, 145–151.
41. Liu,Y.P., Schopman,N.C. and Berkhout,B. (2013) Dicer-independent processing of short hairpin RNAs. *Nucleic Acids Res.*, **41**, 3723–3733.
42. ter Brake,O., Konstantinova,P., Ceylan,M. and Berkhout,B. (2006) Silencing of HIV-1 with RNA interference: a multiple shRNA approach. *Mol. Ther.*, **14**, 883–892.
43. Landthaler,M., Gaidatzis,D., Rothballer,A., Chen,P.Y., Soll,S.J., Dinic,L., Ojo,T., Hafner,M., Zavolan,M. and Tuschl,T. (2008) Molecular characterization of human Argonaute-containing ribonucleoprotein complexes and their bound target mRNAs. *RNA*, **14**, 2580–2596.
44. Prentoe,J. and Bukh,J. (2011) Hepatitis C virus expressing flag-tagged envelope protein 2 has unaltered infectivity and density, is specifically neutralized by flag antibodies and can be purified by affinity chromatography. *Virology*, **409**, 148–155.
45. Sun,G., Li,H. and Rossi,J.J. (2007) Cloning and detecting signature microRNAs from mammalian cells. *Methods Enzymol.*, **427**, 123–138.
46. Das,A.T., Verhoef,K. and Berkhout,B. (2004) A conditionally replicating virus as a novel approach toward an HIV vaccine. *Methods Enzymol.*, **388**, 359–379.
47. Verhoef,K., Marzio,G., Hillen,W., Bujard,H. and Berkhout,B. (2001) Strict control of human immunodeficiency virus type 1 replication by a genetic switch: Tet for Tat. *J. Virol.*, **75**, 979–987.
48. Omoto,S. and Fujii,Y.R. (2005) Regulation of human immunodeficiency virus 1 transcription by nef microRNA. *J. Gen. Virol.*, **86**, 751–755.
49. Ha,M. and Kim,V.N. (2014) Regulation of microRNA biogenesis. *Nat. Rev. Mol. Cell. Biol.*, **15**, 509–524.
50. Starega-Roslan,J., Krol,J., Koscianska,E., Kozlowski,P., Szlachcic,W.J., Sobczak,K. and Krzyzosiak,W.J. (2011) Structural basis of microRNA length variety. *Nucleic Acids Res.*, **39**, 257–268.
51. Mizutani,T., Ishizaka,A., Suzuki,Y. and Iba,H. (2014) 7SK small nuclear ribonucleoprotein complex is recruited to the HIV-1 promoter via short viral transcripts. *FEBS Lett.*, **588**, 1630–1636.
52. Aboul-ela,F., Karn,J. and Varani,G. (1996) Structure of HIV-1 TAR RNA in the absence of ligands reveals a novel conformation of the trinucleotide bulge. *Nucleic Acids Res.*, **24**, 3974–3981.
53. Huthoff,H., Girard,F., Wijmenga,S.S. and Berkhout,B. (2004) Evidence for a base triple in the free HIV-1 TAR RNA. *RNA*, **10**, 412–423.

54. Zacharias,M. and Hagerman,P.J. (1995) The bend in RNA created by the trans-activation response element bulge of human immunodeficiency virus is straightened by arginine and by Tat-derived peptide. *Proc. Natl. Acad. Sci. U.S.A.*, **92**, 6052–6056.
55. Puglisi,J.D., Tan,R., Calnan,B.J., Frankel,A.D. and Williamson,J.R. (1992) Conformation of the TAR RNA-arginine complex by NMR spectroscopy. *Science*, **257**, 76–80.
56. Zhang,Q., Sun,X., Watt,E.D. and Al-Hashimi,H.M. (2006) Resolving the motional modes that code for RNA adaptation. *Science*, **311**, 653–656.
57. Herrera-Carrillo,E., Harwig,A., Liu,Y.P. and Berkhout,B. (2014) Probing the shRNA characteristics that hinder Dicer recognition and consequently allow Ago-mediated processing and AgoshRNA activity. *RNA*, **20**, 1410–1418.
58. Chiang,H.R., Schoenfeld,L.W., Ruby,J.G., Auyeung,V.C., Spies,N., Baek,D., Johnston,W.K., Russ,C., Luo,S., Babiarz,J.E. *et al.* (2010) Mammalian microRNAs: experimental evaluation of novel and previously annotated genes. *Genes Dev.*, **24**, 992–1009.
59. Lee,L.W., Zhang,S., Etheridge,A., Ma,L., Martin,D., Galas,D. and Wang,K. (2010) Complexity of the microRNA repertoire revealed by next-generation sequencing. *RNA*, **16**, 2170–2180.
60. Manzano,M., Forte,E., Raja,A.N., Schipma,M.J. and Gottwein,E. (2015) Divergent target recognition by coexpressed 5'-isomiRs of miR-142-3p and selective viral mimicry. *RNA*, **21**, 1606–1620.
61. Gromak,N., Dienstbier,M., Macias,S., Plass,M., Eyras,E., Caceres,J.F. and Proudfoot,N.J. (2013) Drosha regulates gene expression independently of RNA cleavage function. *Cell. Rep.*, **5**, 1499–1510.
62. Zamudio,J.R., Kelly,T.J. and Sharp,P.A. (2014) Argonaute-bound small RNAs from promoter-proximal RNA polymerase II. *Cell*, **156**, 920–934.
63. Xie,M., Li,M., Vilborg,A., Lee,N., Shu,M.D., Yartseva,V., Sestan,N. and Steitz,J.A. (2013) Mammalian 5'-capped microRNA precursors that generate a single microRNA. *Cell*, **155**, 1568–1580.
64. Chiu,Y.L., Coronel,E., Ho,C.K., Shuman,S. and Rana,T.M. (2001) HIV-1 Tat protein interacts with mammalian capping enzyme and stimulates capping of TAR RNA. *J. Biol. Chem.*, **276**, 12959–12966.
65. Chiu,Y.L., Ho,C.K., Saha,N., Schwer,B., Shuman,S. and Rana,T.M. (2002) Tat stimulates cotranscriptional capping of HIV mRNA. *Mol. Cell*, **10**, 585–597.